CORROSION SCIENCE AND TECHNOLOGY, Vol.19, No.1(2020), pp.16~22
[Research Paper]
pISSN: 1598-6462 / eISSN: 2288-6524
DOI: https://doi.org/10.14773/cst.2020.19.1.16

The Influence of Hydrotalcite Intercalated with Benzoate on UV Stability of Acrylic Coating

Thuy Duong Nguyen[1], Anh Son Nguyen[1], Thu Thuy Thai[1], Gia Vu Pham[1], Thi Xuan Hang To[1,2,†], and Marie-Georges Olivier[3]

[1]*Institute for Tropical Technology, Vietnam Academy of Science and Technology 18 Hoang Quoc Viet, Cau Giay, Hanoi, Vietnam*
[2]*Graduate University of Science and Technology, Vietnam Academy of Science and Technology, 18 Hoang Quoc Viet, Cau Giay, Hanoi, Vietnam*
[3]*Université de Mons (UMONS), Faculty of Engineering, Materials Science Department 20 Place du Parc, Mons, Belgium*

(Received January 05, 2020; Revised February 04, 2020; Accepted February 05, 2020)

It is important to realize that benzoate was intercalated into hydrotalcite (HTC-Bz) by the co-precipitation method. In this case, acrylic coating with 0.5 wt% HTC-Bz was deposited on carbon steel using the spin coating method. Next, the HTC-Bz structure was characterized by Field emission scanning electron microscopy (FESEM), X-ray diffraction (XRD), and Fourier transform infrared spectroscopy (FT-IR). In fact, an ultraviolet vision spectroscopy (UV-Vis) was used to determine the benzoate content in HTC-Bz, and the UV absorption ability of HTC-Bz. Using electrochemical techniques, water contact angle measurement, and thermal-gravimetric analysis, we compared the protective properties before and after QUV test, hydrophobicity and the thermal stability of acrylic coating containing HTC-Bz. The obtained results showed that HTC-Bz with a plate-like structure was successfully synthesized; benzoate was intercalated into the interlayer of hydrotalcite with a concentration of 28 wt%. Additionally, it was noted that HTC-Bz has an UV absorption peak at 225 nm. In conclusion, the addition of HTC-Bz enhanced the UV stability, hydrophobicity and the thermal stability of acrylic coating.

Keywords: *Benzoate, Hydrotalcite, Acrylic coatings, UV stability*

1. Introduction

Acrylic coatings are interesting to scientists and manufacturers because of good properties such as weather resistance, mechanical strength and high chemical resistance. They are often used as a top coating in paint systems for outdoor conditions. Solvent based acrylic coatings are often used on steel structures, fuel tanks and auto parts [1,2]. In recent years, environmentally friendly coatings such as weather-durable coatings have been investigated to minimize environmental pollution. Organic coating systems are often degraded rapidly by environmental factors such as ultraviolet rays, heat and humidity. Among these factors, ultraviolet rays are the main factor causing the degradation of coating properties such as cracks, delamination, discoloration and change of mechanical properties [3]. To enhance the durability of the coating exposed to UV radiation conditions, the organic/inorganic UV absorbers such as benzophenone cinnamic acid, 2,4-dihydroxybenzophenone-5-sulfonate [4-6], titanium dioxide (TiO_2), zinc oxide (ZnO), graphene oxide (GO) [7-9] were added to the coatings. Inorganic nano-sized additives are usually more durable but the size of these nanoparticles must be smaller than the wavelength of the visible region (400 nm - 800 nm). Organic additives with low molecular weight are not fixed in the polymer matrix and leak easily from the coating, which leads to changing UV stability of coatings. To resolve this issue, light stabilizers or organic UV absorbers are inserted in materials with lamellar structure, as hydrotalcites [10,11].

Hydrotalcites, known as anion clay, have structures consisted of positive charge hydroxide layer and exchangeable anions in the interlayer. With anion exchange capacity, they can be modified with different anions and applied in many fields due to their flexible properties. Hydrotalcites can be used as absorbents, catalyst precursors, drug containers, corrosion inhibitor con-

†Corresponding author: ttxhang60@gmail.com

tainers and light stabilizers in polymers [11-15]. In recent years, there are many researches focused on the use of hydrotalcites as additives for polymers coating to enhance the protective properties of coatings, anti-ultraviolet ability of coatings and thermal stability of coating [16,17]. The hydrotalcites, with brucite-like layer structures, have large surface area, so they can cover surface of coating better than common inorganic nano-sized additives. The hydrotalcites have been modified with UV absorbers, light stabilizers such as dodecylsulfate, 2,4-dihydroxybenzophenone-5-sulfonate, 3,4-dihydroxycinnamic acid, p-aminobenzoic acid, derivatives of benzoic acid and hindered amine light stabilizer (HALS) [6,11,18-21]. Combinations of hydrotalcites and 2,4-dihydroxybenzophenone-5-sulfonate or derivatives of benzoic acid give higher thermal stability and better UV absorption capacity [6,20]. In several coatings (propylene, polyvinyl chloride), the presence of hydrotalcites containing UV stabilizers enhanced the stability of these coatings. The hydrotalcite intercalated with hindered amine light stabilizer (HT-HALS) improved the light stability and reduced the rate of photo-oxidation of propylene film [11,21]. The hydrotalcite intercalated with 2-hydroxy-4-methoxybenzophenone-5-sulfonic acid enhanced the thermal and weather stability of polyvinyl chloride [22].

In previous studies, hydrotalcite containing benzoate was used as an anti-corrosion additive in the epoxy coating for corrosion protection of carbon steel [23-24]. Benzoate has both corrosion inhibition and ultraviolet absorption ability, therefore hydrotalcite intercalated with benzoate can be used as UV absorber for organic coatings. This work aims to study the effect of hydrotalcite intercalated with benzoate on UV and thermal stability of acrylic coating. Hydrotalcite intercalated with benzoate (HTC-Bz) was fabricated by the co-precipiation method and characterized by FESEM, XRD, FT-IR, UV-Vis. The influence of HTC-Bz on the UV resistance, hydrophobicity, thermal stability of acrylic coatings was evaluated by electrochemical techniques, water contact angle measurement, and thermal-gravimetric analysis. The surface of coatings was observed by SEM.

2. Experimental Methods

2.1 Materials

Aluminum nitrate nonahydrate ($Al(NO_3)_3.9H_2O$) (98%), Zinc nitrate hexahydrate ($Zn(NO_3)_2.6H_2O$) (98%) from Sigma Aldrich were used for fabrication of hydrotalcite. Sodium benzoate ($C_7H_5O_2Na$) (99%) from VWR is used as an organic compound.

XC 35 carbon steel was used as the substrate. The dimension of steel plates was 15 cm × 10 cm × 0.2 cm. Before application of coatings, the steel sheets were polished with abrasive papers from grade 80 to 400, cleaned with ethanol and then dried.

For preparation of acrylic coating, Dianal BR-116 solid acrylic resin with an equivalent weight of 45000 g/eq from Misubishi was used. Dianal BR-116 particles were dissolved in xylene (60% xylene).

2.2 Fabrication of hydrotalcite laminated by benzoate

Hydrotalcite laminated by benzoate (HTC-Bz) was fabricated by the co-precipitation reaction. Solution A is a salt mixture of $Zn(NO_3)_2$ and $Al(NO_3)_3$ (molar ratio of Zn^{2+}/Al^{3+} = 2/1). Solution B is a mixture of two solutions: benzoate solution and sodium hydroxide solution. Solution B was kept under nitrogen atmosphere at room temperature and pH = 8 – 9. Solution A was added to solution B with vigorous stirring. Then slurry was kept at 50 °C for 24 h under nitrogen atmosphere. The white precipitation formed was washed with large amounts of degassed distilled water before drying at a temperature of 70 °C for 24 h.

The schematic diagram of chemical reaction process of hydrotalcite laminated by benzoate is as following:

$$\text{Zn(II)+ Al(III) + Benzoate} \xrightarrow[\text{pH=8-10}]{\text{NaOH}} \text{Precipitates} \xrightarrow{\text{Aging}} \text{HTC-Bz}$$

2.3 Preparation of acrylic coating containing hydrotalcite laminated by benzoate

Acrylic resin was dissolved in xylene. HTC-Bz was dispersed in acrylic resin with a concentration of 0.5 wt% by stirring for 30 min and then sonicated with ultrasonics for 15 min and finally stirred for 24 h. The spin coating method was used to deposit acrylic coatings on the cleaned steel substrate. These coatings were dried at room temperature for 30 days. The thickness of dried coatings was 30 ± 5 μm (measured by Minitest 600 Erichen digital meter).

2.4 Characterization

Powder X-ray diffraction patterns of hydrotalcite (HTC) and hydrotalcite laminated by benzoate (HTC-Bz) were obtained on Siemens diffractometer D5000 using CuKα radiation (λ = 0.15406 nm) at room temperature from 1° to 70° with scanning speed of 2.6 °/min under air conditions.

Fourier transform infrared spectra of HTC and HTC-Bz powder were measured on Nexus 670 Nicolet spectrometer with resolution at 32 cm^{-1} using the KBr method

with transmission mode. The spectra were obtained in the region of 400 - 4000 cm^{-1}.

Field emission scanning electron microscope of HTC-Bz powder and coatings surface was operated on FESEM Hitachi S-4800 at a voltage of 5.0 kV.

UV-Vis spectroscopy was used to determine the content of benzoate in HTC-Bz and UV absorption ability of HTC-Bz. The amount of benzoate in HTC-Bz was determined by the following protocol: 0.03 g of HTC-Bz was dissolved in 1.2 mL of 1 M HCl solution in 50-mL volumetric flask. Then distilled water was filled into the balance of volumetric flask. The absorbance of benzoate was monitored by UV–Vis spectrophotometer at λ_{max} = 225 nm. Based on the benzoate standard curve, the content of benzoate into the HTC-Bz was calculated. The standard curve was obtained from a series of benzoate standard solutions.

The UV absorption ability of HTC-Bz was analyzed by UV-Vis spectra (GBC Cintra 40 spectrometer) in distilled water at 0.1 wt%. The wavelength region was in the range of 200 - 400 nm.

2.5 UV exposure evaluations

QUV test

QUV test was carried out in UV-condensation chamber (ATLAS UVCON UC-327-2). The test was done following ASTM standard G 53-96 (1 cycle period was 8 h of UV exposure at 60 °C followed by 4 h of condensation at 50 °C). The test was carried out continuously, repeating the cycle. The properties of exposed samples were evaluated after 4 cycles and 8 cycles, respectively. For each system, 3 samples were tested.

Electrochemical impedance measurements

Electrochemical impedance measurement was used to investigate the protection performance of the acrylic coating containing HTC-Bz before and after QUV test. Electrochemistry impedance measurements were carried out on a Biologic SP300. Before each electrochemistry impedance test, the samples were immersed in 3% Na_2SO_4 solution for 1 h. This protocol was set up in a frequency range of 100 kHz to 10 mHz. We used a three-electrode system including painted steel as working electrode, saturated calomel (SCE) as reference and platinum grid as counter electrode. For each experiment, three samples were measured.

2.6 Hydrophobicity test

To test the hydrophobicity of acrylic coating, contact angle measurements were done. The water contact angle of coating was determined by a self-developed goniometer combined with a high resolution camera. Measurements were carried out in an ambient atmosphere at room temperature. The volume of the applied droplets of distilled water is 5 μL. Contact angle (θ) was determined according to the following equation: $\tan(\theta/2) = 2h/d$

where h is the droplet height and d is the base diameter.

The droplet height and the base diameter were measured from the optical images of the water droplet. Five measurements were made on different parts of the surface, and the average contact angle value was recorded.

2.7 TGA measurements

The thermal stability of acrylic coatings was tested using the thermal-gravimetric analysis (TGA). The test was controlled by a computer at a heating rate of 10 °C/min under air atmosphere in the range of 30 - 900 °C. The sample weight was about 10 - 11 mg.

3. Results

3.1 Morphology and structure of HTC-Bz

The morphology and structure of HTC-Bz were observed and examined by SEM, XRD and FT-IR. Fig. 1 shows the scanning electron micrograph of HTC-Bz. SEM image displays a sheet-like morphology of hydrotalcites. HTC-Bz crystals were thin, flat and the sizes of these plates was in the range of 200 - 500 nm.

Fig. 2 presents the XRD patterns of HTC and HTC-Bz. The XRD patterns of both hydrotalcites show typical characteristic diffraction peaks of (003), (006) and (110) of layered materials. The (003) diffraction peak of HTC is observed at 2-theta = 11.7° corresponding to d spacing of 7.74 Å, which is similar to the reported value of hydro-

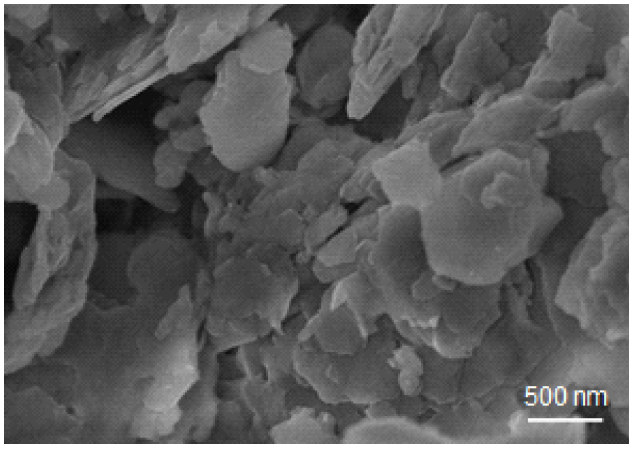

Fig. 1 SEM photograph of HTC-Bz.

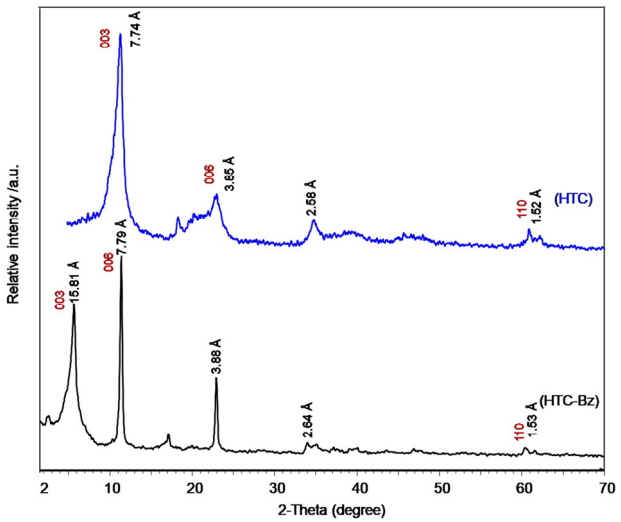

Fig. 2 XRD patterns of HTC and HTC-Bz.

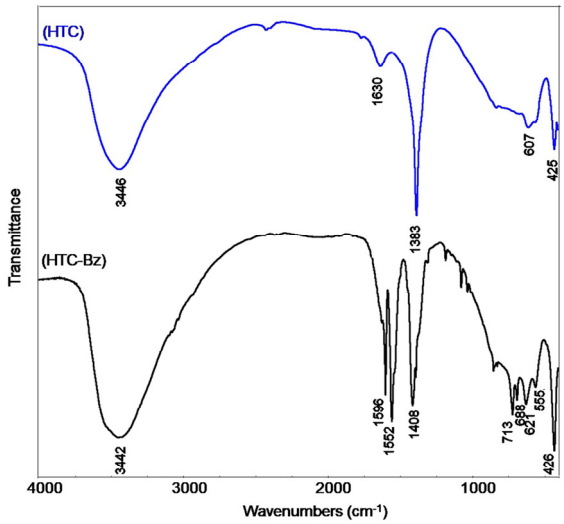

Fig. 3 FT-IR spectra of HTC and HTC-Bz.

talcite [24]. XRD pattern of HTC-Bz shows the (003) plane and (006) plane reflections at 2-theta = 5.6°, 11.4° corresponding to d spacing of 15.81 and 7.79 Å, respectively [25]. In comparison to synthesized pure hydrotalcite, the peak of (003) plane reflection shifted to lower value of 2-theta. It is likely that the increase of d spacing was caused by the intercalation of benzoate anion into HTC-Bz structure.

FT-IR spectra of HTC and HTC-Bz are presented in Fig. 3. The FT-IR spectrum of HTC displayed the characteristic bands of Zn-O, Al-O, NO_3^- group and water molecules in the interlayer domain at 425 cm^{-1}, 607 cm^{-1}, 1383 cm^{-1} and 1630 cm^{-1}, respectively [24]. In the case of HTC-Bz, FT-IR spectrum shows the characteristic peaks of both hydrotalcite and benzoate. A strong vibration band at the 3442 cm^{-1} is assigned to the stretching vibration of OH group into water molecules and hydroxide basal layers. The characteristic bands at 621 cm^{-1} and 426 cm^{-1} correspond to Al-O and Zn-O vibration [6]. The absorption bands at 1552 cm^{-1} and 1408 cm^{-1} are ascribed to C-O and -COOH group into benzoate structure. The peaks at 1596 cm^{-1} and 713 cm^{-1} are assigned to aromatic ring of benzoate [24,25]. The characteristic bands of both benzoate and hydrotalcite appear in spectrum of HTC-Bz. The FTIR results suggest the presence of benzoate into HTC-Bz structure.

Based on the UV-Vis analysis data, the amount of benzoate into HTC-Bz was determined. The calibration curve determined from a series of benzoate standards solutions. From the calibration curve, the relationship between the absorbance and the concentration was: $A = 8236\ C_{Bz} - 0.012103$ with $R^2 = 0.99898$ (C_{Bz} is the concentration of benzoate (mol/l) and A is the absorbance). From the UV-Vis curve of the solution containing HTC-Bz reacting with HCl, absorbance A was determined to calculate concentration C_{Bz}. The Bz loading in HTC-Bz is about 28 wt%. The obtained result is close to reported works (benzoate amount into modified hydrotalcite were about 26-27%) [24,25].

Fig. 4 illustrates the UV-Vis absorbance curve of HTC-Bz dispersed in distilled water with concentration 0.1 wt%. The max absorption peak of HTC-Bz at about 225 nm corresponds to π-π bond of benzene rings, hydrogen bonding and electrostatic attraction between hydrotalcite and benzoate. The result showed that HTC-Bz can absorb UV light in the range from 200 nm to 400 nm. Compared to literatures, hydrotalcites intercalated with or-

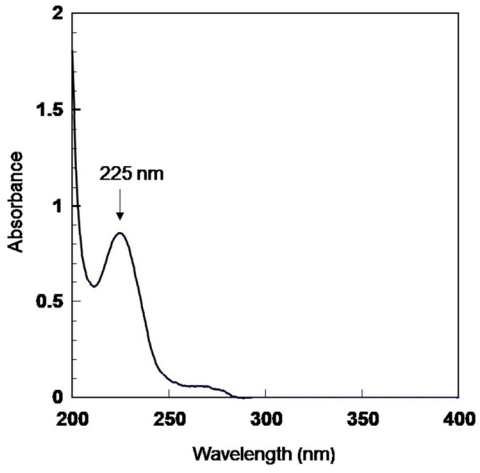

Fig. 4 UV-Vis spectrum of HTC-Bz solution.

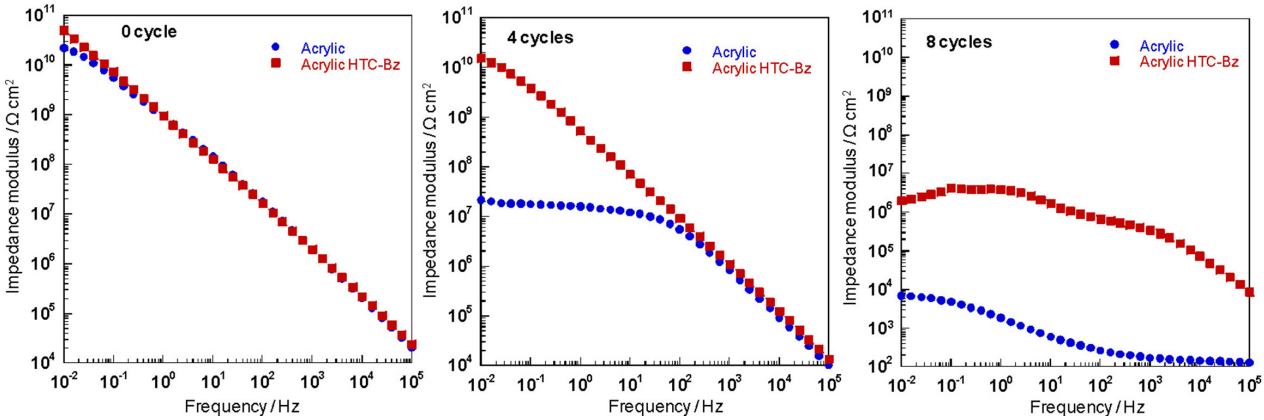

Fig. 5 Impedance diagrams of pure acrylic coatings and acrylic coating + HTC-Bz before and after QUV exposure.

ganic UV absorbers exhibited the same UV absorption ability in this region [6,21,22].

3.2 UV stability of acrylic coatings

The UV stability of acrylic coatings after UV exposure was evaluated and compared to them before exposure by electrochemical impedance measurement. The impedance diagrams in Bode style of blank coating and coating containing HTC-Bz at a concentration of 0.5 wt% before and after different cycles (4 cycles and 8 cycles) of QUV exposure are shown in Fig. 5.

Before exposure, both coatings (blank coatings and coatings containing HTC-Bz) had high impedance modulus values at low frequency (>10^{10} Ω.cm^2). These values were very close to each other. After 4 cycles of exposure, the impedance modulus value of blank coating decreased rapidly. Meanwhile, the impedance modulus value of coating containing HTC-Bz only decreased slightly and remained higher than that of blank coating. After 8 cycles of QUV exposure, impedance modulus value of both coatings decreased and the value of blank coating was lower than that of the coating containing HTC-Bz.

To consider the protective performance of coatings, the impedance modulus at low frequency 100 mHz ($|Z|_{100\ mHz}$) were extracted from impedance diagrams. Fig. 6 shows the $|Z|_{100\ mHz}$ values of blank coating and coating containing HTC-Bz at different exposure times.

Before QUV test, both systems had the high $|Z|_{100\ mHz}$ values (> 10^9 Ω.cm^2). After 4 cycles of QUV exposure, $|Z|_{100\ mHz}$ value of pure acrylic coating rapidly decreased. However, $|Z|_{100\ mHz}$ of acrylic coating with HTC-Bz decreased little compared to that before exposure. After 8 cycles of UV exposure, $|Z|_{100\ mHz}$ value of pure acrylic coating continued to decrease. The decrease of $|Z|_{100\ mHz}$ values can be caused by degradation of coating under UV irradiation. For the acrylic coating containing HTC-Bz, $|Z|_{100\ mHz}$ value decreased but it remained higher than that of the blank coating. The results can be explained by the UV absorption and barrier effect of HTC-Bz [20,24]. The obtained result was similar to reported works [11,17]. Hydrotalcites intercalated with UV absorbers improved the UV stability for polymer coatings.

3.3 Hydrophobicity of acrylic coatings

Hydrophobicity of coatings was examined to study the effect of HTC-Bz on the UV stability of acrylic coating. Fig. 7 shows the water contact angle photos of pure acrylic coating and coating containing HTC-Bz. The contact angle of pure acrylic coating was about 79.9°. When HTC-Bz was added into acrylic coating, the water contact angle of coating increased to 83.9°. It can be due to the presence of hydrophobic aromatic ring (benzoate) and the good bar-

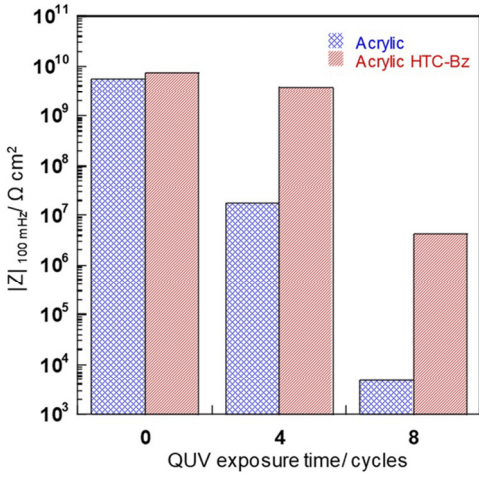

Fig. 6 $|Z|_{100\ mHz}$ values of blank coating and coating containing HTC-Bz at different exposure times.

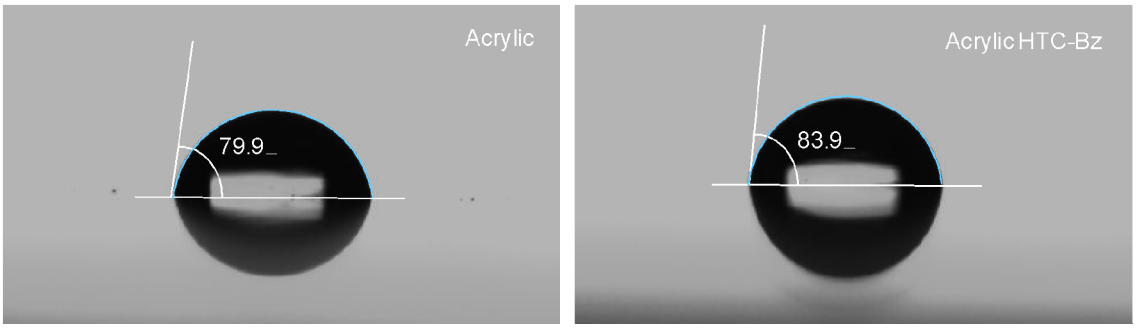

Fig. 7 The water contact angle photos of blank coating and coating containing HTC-Bz.

rier ability of HTC-Bz [24]. The presence of HTC-Bz increased the hydrophobicity of acrylic coating so the protective property of coating was enhanced.

3.4 Surface observation

In order to confirm the effect of HTC-Bz on surface profile of acrylic coating, the morphology of acrylic coatings was observed by SEM. Fig. 8 shows the surface micrographs of acrylic coating and acrylic coatings with HTC-Bz. It can be seen that the pure acrylic coating surface is smooth. The SEM photo of the acrylic coating containing HTC-Bz displays the structure of HTC-Bz on the surface of coating. With layer structure and large surface area, HTC-Bz changed hydrophobicity of acrylic coating.

3.5 Thermal stability of acrylic coatings

Thermal stability of acrylic coatings was studied by TG analysis. Fig. 9 shows the thermal weight loss curves of pure acrylic coating and coating containing HTC-Bz. Results showed that the pure acrylic coating started to lose weight from 192 ºC then continued to lose weight at 306 ºC and stopped at 420 ºC. For the coating containing HTC-Bz, the weight loss point happened at higher temperature (at 319 ºC) in comparison to the blank coating and it stopped at 500 ºC. For the pure acrylic coating,

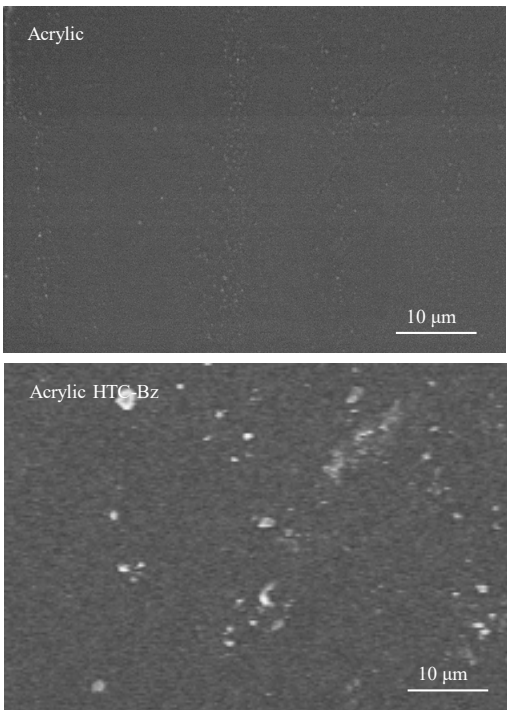

Fig. 8 SEM images of acrylic coating and acrylic coating containing HTC-Bz.

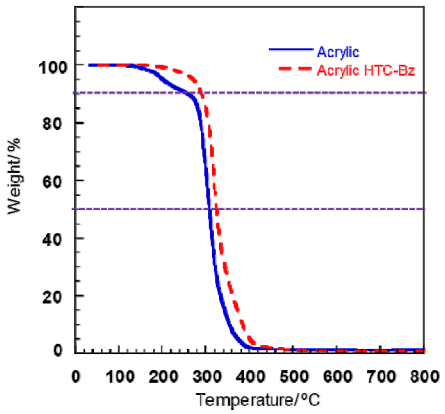

Fig. 9 Thermal weight loss curves of pure acrylic coating and coating containing HTC-Bz.

Table 1 TGA results of pure acrylic coating and acrylic coating containing HTC-Bz

Sample	$T_{10\%}$ (°C)	$T_{50\%}$ (°C)	T_{max} (°C)
Pure acrylic coating	259	308	420
Acrylic coating + HTC-Bz	290	325	500

as shown in Table 1, 10% weight loss temperature and 50% weight loss temperature occurred at 259 ºC and 308 ºC, respectively. Meanwhile, for the coating with HTC-Bz, 10% weight loss temperature and 50% weight loss temperature happened at 290 ºC and 325 ºC. We assumed that thermal decomposition of acrylic coating containing HTC-Bz was retarded due to the thermal stability of HTC-Bz [21,22].

4. Conclusions

Benzoate was successfully intercalated into hydrotalcite by co-precipitation method with the content about 28 wt%. HTC-Bz had plate-like structure and size in the range of 200 - 500 nm. HTC-Bz at a concentration of 0.5 wt% improved the UV stability of acrylic coating. After 8 cycles of UV exposure, the impedance modulus value at low frequency 100 mHz of the acrylic coating containing HTC-Bz was still very high (>10^6 Ω.cm^2). The hydrophobicity and thermal stability of acrylic coating were also enhanced with the addition of HTC-Bz.

Acknowledgments

The authors gratefully acknowledge the financial support of Vietnam Academy of Science and Technology for young researchers.

References

1. P. Kotlík, K. Doubravová, J. Horálek, L. Kubáč, and J. Akrman, *J. Cult. Herit.*, **15**, 44 (2014).
2. T. V. Nguyen, X. H. Le, P. H. Dao, C. Decker, and P. Nguyen-Tri, *Prog. Org. Coat.*, **124**, 137 (2018).
3. D. Kotnarowska, *Journal of Surface Engineered Materials and Advanced Technology*, **8**, 95 (2018).
4. A. C. T. Cursino, F. da Lisboa, A. dos Pyrrho, V. P. de Sousa, and F. Wypych, *J. Colloid Interf. Sci.*, **397**, 88 (2013).
5. Y. Li, L. Tang, X. Ma, X. Wang, W. Zhou, and D. Bai, *J. Phys. Chem. Solids*, **107**, 62 (2017).
6. S. Li, Y. Shen, M. Xiao, D. Liu, L. Fa, and K. Wu, *J. Ind. Eng. Chem.*, **20**, 1280 (2014).
7. H. Aziz and F. Ahmad, *Prog. Org. Coat.*, **101**, 431 (2016).
8. A. M. E. Saeed, M. A. El-Fattah, and A. M. Azzam, *Dyes Pigm.*, **121**, 282 (2015).
9. N. Nuraje, S. I. Khan, H. Misak, and R. Asmatulu, *ISRN Polymer Sci.*, 8 pages (2013).
10. A. A. Marek, V. Verney, G. Totaro, L. Sisti, A. Celli, and F. Leroux, *J. Solid State Chem.*, **268**, 9 (2018).
11. Q. Zhang, F. Leroux, P. Tang, D. Li, and Y. J. Feng, *Polym. Degrad. Stab.*, **154**, 55 (2018).
12. H. Zhou, Z. Jiang, and S. Wei, *Appl. Clay Sci.*, **153**, 29 (2018).
13. U. Costantino, M. Curini, F. Montanari, M. Nocchetti, and O. Rosati, *Micropor. Mesopor. Mat.*, **107**, 16 (2008).
14. V. Rives, M. Arco, and C. Martin, *Appl. Clay Sci.*, **88-89**, 239 (2014).
15. J. Tedim, S. K. Poznyak, A. Kuznetsova, D. Raps, T. Hack, M. L. Zheludkevich, and M. G. S. Ferreira, *ACS Appl. Mater. Interfaces*, **2**, 1528 (2010).
16. B. Pilch-Piteraa, M. K¸edzierskib, E. Olejnikc, and S. Zapotoczny, *Prog. Org. Coat.*, **95**, 120 (2016).
17. S. Aisawaa, C. Nakada, H. Hirahara, N. Takahashi, and E. Narita, *Appl. Clay Sci.*, **180**, 105205 (2019).
18. S. M. Mohsin, M. Z. Hussein, S. H. Sarijo, S. Fakurazi, P. Arulselvan, and Y. H. Taufiq-Yap, *J. Biomed Nanotechnol.*, **10**, 1490 (2014).
19. S. B. Khan, C. Liu, E.S. Jang, K. Akhtar, and H. Han, *Mater. Lett.,* **65**, 2923 (2011).
20. A. C. T. Cursino, J. E. F. C. Gardolinski, and F. Wypych, *J. Colloid Interf. Sci.*, **347**, 49 (2010).
21. R. Ma, M. Zhao, Y. Mo, P. Tang, Y. Feng, and D. Li, *Appl. Clay Sci.*, **180**, 105196 (2019).
22. X. Zhang, L. Zhou, H. Pi, S. Guo, and J. Fu, *Polym. Degrad. Stabil.*, **102**, 204 (2014).
23. T. D. Nguyen, T. X. H. To, J. Gervasi, Y. Paint, M. Gonon, and M.-G. Olivier, *Prog. Org. Coat.*, **124**, 256 (2018).
24. T. D. Nguyen, T. X. H. To, A. Nicolay, Y. Paint, and M.-G. Olivier, *Prog. Org. Coat.*, **101**, 331 (2016).
25. Y. Wang, and D. Zhang, *Mater. Res. Bull.*, **46,** 1963 (2011).